Paper 2

An insight into the Bucaramanga nest

Zoya Zarifi, Jens Havskov and Andrzej Hanyga

In revision in Tectonophysics, 2006

2. An insight into the Bucaramanga nest

Zoya Zarifi, Jens Havskov and Andrzej Hanyga

(Zoya.Zarifi@geo.uib.no; Jens.Havskov@geo.uib.no;Andrzej.Hanyga@geo.uib.no)

Department of Earth Science , University of Bergen, Allegaten 41, 5007 Bergen, NORWAY

2.1. Abstract

We used the local seismicity for the period 1993-2001, in the north east of Colombia to show the existence of two slabs in the north and south of the Bucaramanga nest. The northern slab has a dip angle of about 25° and the southern slab has a 50°dip angle, while the dip in the Bucaramanga nest is about 29°. In order to explain the nature of the Bucaramanga nest, we proposed the scenario of collision between these two slabs. Using a 3D Finite Element Model (FEM) we show that collision can perturb, modify and concentrate the stress field. The active process of dehydration embrittelment at intermediate depth and the concentrated stress field in the collision zone may explain the nature of the Bucaramanga nest. The perturbed and modified stress field resulting from the simultaneous effect of collision and subduction can explain the variation in the focal mechanism and the complexity in the source of the earthquakes in the Bucaramanga nest.

Keywords: Bucaramanga nest, Collision, Concentrated stress field, Stress inversion

2.2. Introduction

In some subduction zones and at intermediate depths, unusual dense seismic activity has been observed. This kind of activity has been labeled seismic nests. A seismic nest

is defined by high stationary activity relative to its surroundings. Within this definition, two classes of nests can be defined: (A) nests related to tectonic processes in the subduction zones like Vrancea in Romania, Hindu Kush in Afghanistan and Bucaramanga in Colombia (Zarifi & Havskov, 2003) and (B) nests located on down-going slabs and related to volcanic activity like in central America (Carr & Stoiber, 1973), in New Zealand (Blot, 1981*a*), in New Hebrides (Blot, 1981*b*) and in the Aleutian (Engdahl, 1977).

The present study aims to explain the processes associated with the class (A), in the Bucaramanga nest. The Bucaramanga nest is located in the north east of Colombia and centered at $6.8°N$ and $73.1°W$ at intermediate depth (about 155km) (Tryggvason & Lawson, 1970; Schneider *et al.*, 1987; Frohlich *et al.*, 1995; Ojeda & Havskov, 2001; Zarifi & Havskov, 2003). The Bucaramanga nest differs from the other nests by its high rate of activity in a volume much smaller than the other nests at intermediate depth in the same class (Schneider *et al.*, 1987; Zarifi & Havskov, 2003). There have been many attempts to explain the nature of this nest (Schneider *et al.*, 1987; Shih *et al.*, 1991; Van der Hilst & Mann, 1994; Cortes & Angelier, 2005), however there are still unresolved problems. These are related to the complexity of the tectonic process in this area and the lack of enough local data to define clearly the plate geometry. Colombia exhibits a complex deformation with convergence of four plates (Taboada *et al.*, 2000; Malave & Suarez, 1995; Van der Hilst & Mann, 1994). The North Andes block as part of the south American plate, the Panama block, the Caribbean and the Nazca plates (Figure 1).

Tomographic investigations of the complex structure of the upper mantle below the northeastern south America (Van der Hilst & Mann, 1994) have revealed two slabs beneath Colombia and western Venezuela. According to Van der Hilst & Mann (1994), the northern slab with a dip angle of $17°$ reaches to a depth of 275 km and correlates with the subducted late cretaceous oceanic plateau of the Caribbean plate. Farther south, a second slab, with a dip angle of $50°$ reaches to a depth of at least 500 km and corre-

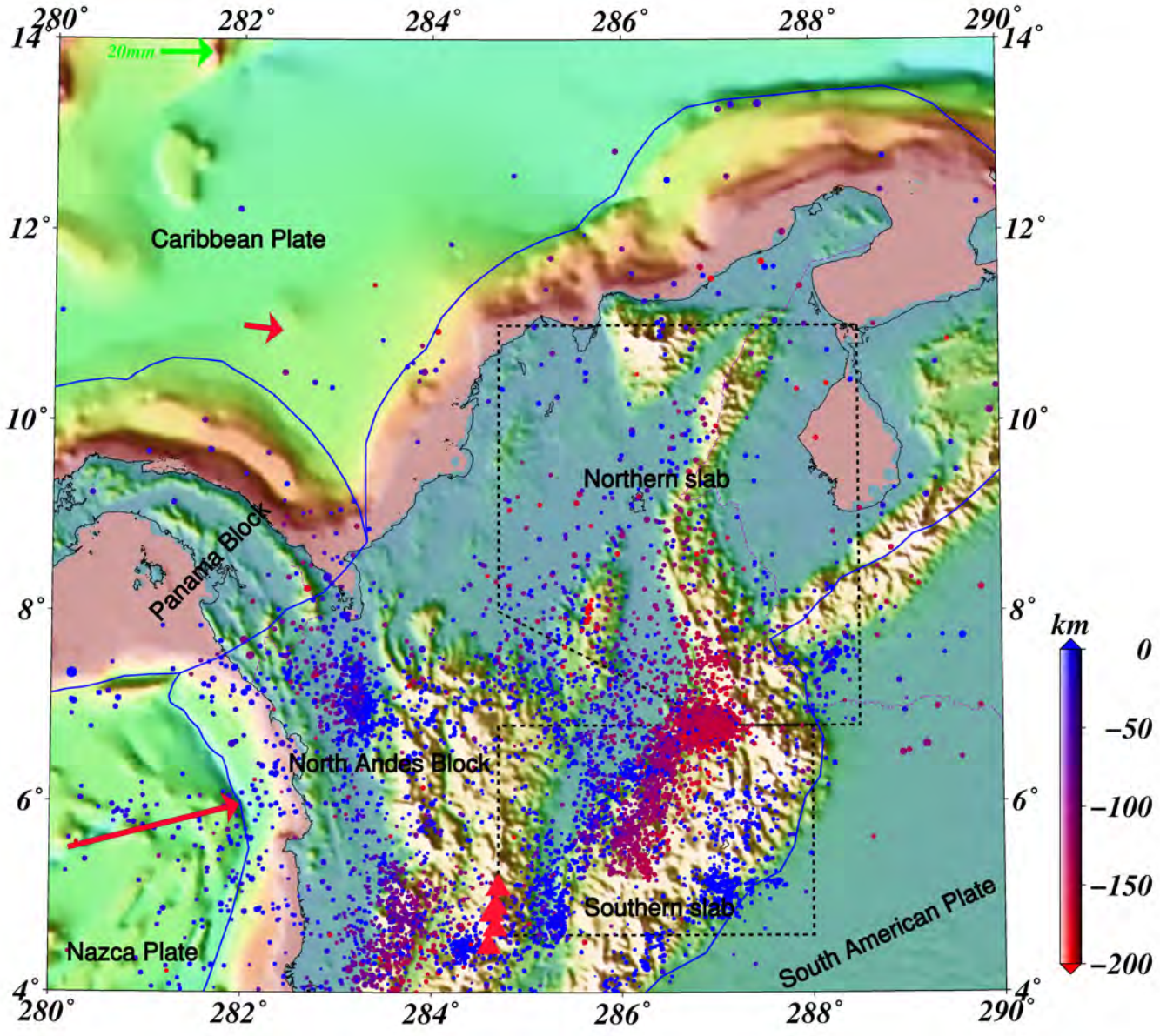

Figure 1: The tectonic, seismic and volcanic setting of Colombia. The North Andes block is considered to be stationary relative to Nazca and Caribbean plates. The colored dots are the location of the local earthquakes form National Network of Colombia, the red triangles show the locations of the volcanoes.Thick blue line show the boundary of the plates (Bird, 2003). The red arrows show the direction of convergence based on NUVEL-1 model (De Mets *et al.*, 1990) and the green arrow is the scale. The dot lines show the approximate location of the two slabs in northeast Colombia.

lates to the subducted oceanic crust of the Nazca plate. Based on Van der Hilst & Mann (1994) research, the Bucaramanga nest appears to be located within the southern slab on the top with an average dip direction of $109°$, where the mantle wedge below the nest is marked by P-wave velocity that is more than 2.5% lower than the average velocity at that depth. According to the same authors, this low velocity wedge becomes less pronounced towards the north and may support the hypothesis that the Bucaramanga nest is being produced by partial melting and rising of magma accompanying the formation of a volcanic arc (Schneider *et al.*, 1987; Shih *et al.*, 1991). However they could not reject the possibility that the nest could be produced by a complex stress field near the contact of two the slabs. On the other hand Chen *et al.* (2001) have suggested that the volcanism and intermediate depth seismicity in the Nazca plate, show no direct correlation. Also, no volcanic activity can be associated to the Caribbean slab. This can be a hint to the validity of the suggested scenario by Schneider *et al.* (1987) and Shih *et al.* (1991) as an explanation of the nature of the Bucaramanga nest.

Since 1993 a local network has been in operation in Colombia (Ojeda & Havskov, 2001). This network has a much lower detection threshold (2.5 Ml) than the global networks, so a large amount of data has been recorded by high location accuracy. We use this data set, the Harvard CMT solution and a 3D numerical simulation using Finite Element Method (FEM) to explain a possible reason behind the nature of the Bucaramanga nest.

2.3. Seismicity

All the earthquakes in the time period from 1993 to 2001 reported by the National Seismic Network of Colombia are shown in Figure 1. We studied these data to show the existence of two slabs with two different dip angles and dip directions in the northeast of Colombia. The original data in this area were located by HYPO71 (Lee & Lahr, 1987) and then were relocated by an improved velocity model (Ojeda & Havskov, 2001) using HYPOCENTER (Lienert & Havskov, 1995). In order to improve the accuracy of

the locations, we relocated some subsets of these data using HYPODD (Waldhauser & Ellsworth, 2000; Waldhauser, 2001). The results did not show any pronounced difference compared to the data relocated with HYPOCENTER. Since using of HYPODD restricts our choices of stations location, some data would be lost and the size of the nest and the seismicity in south and north of the area of interest ($4^\circ - 14^\circ N$ and $80^\circ - 70^\circ W$) would not be clearly defined. Therefore we decided to use the data relocated with HYPOCENTER. These data confirm the existence of two slabs with two different dips, meeting in the area of the Bucaramanga nest. It can be seen (Figure 1) that in the area between $75^\circ - 72^\circ W$ and $4^\circ - 10^\circ N$ the rate of seismic activity is higher than in the other parts in the North Andes block and clearly the Bucaramanga nest can be recognized with its dense seismicity. In order to have an idea about the geometry of the nest, we collected the data using the following criteria: RMS of travel time residuals less than 0.7 and a maximum error in latitude, longitude and depth of 15 km. The result shows that the Bucaramanga nest has elliptical shape with the major axes elongated in almost $W - E$ direction with the size of 27 km. The minor axis is around 15 km. The nest is centered at $6.8^\circ N$ and $73.08 \pm .02^\circ W$ in depth around 155 km. The thickness of nest is about 25 km and is elongated about 37 km in down dip direction (Figure 3).

We made different 2D profiles to investigate the dip angle of the slabs and the Bucaramanga nest. The results show that the dip angle of the northern slab is about $25^\circ$and the dip direction is about 130°. In the south the dip angle is about 50°, and the dip direction changes from about 80° close to the nest to about 110° towards the south. The dip angle in the area of the nest is about 29°.

Figures 2 and 3 show 3D views of the area $80^\circ - 70^\circ W$ and $4^\circ - 10^\circ N$. These figures also clearly show the difference in the seismicity and in the dip angle of the slabs in the north and the south and confirm the existence of different slabs with different seismic activity in this area.

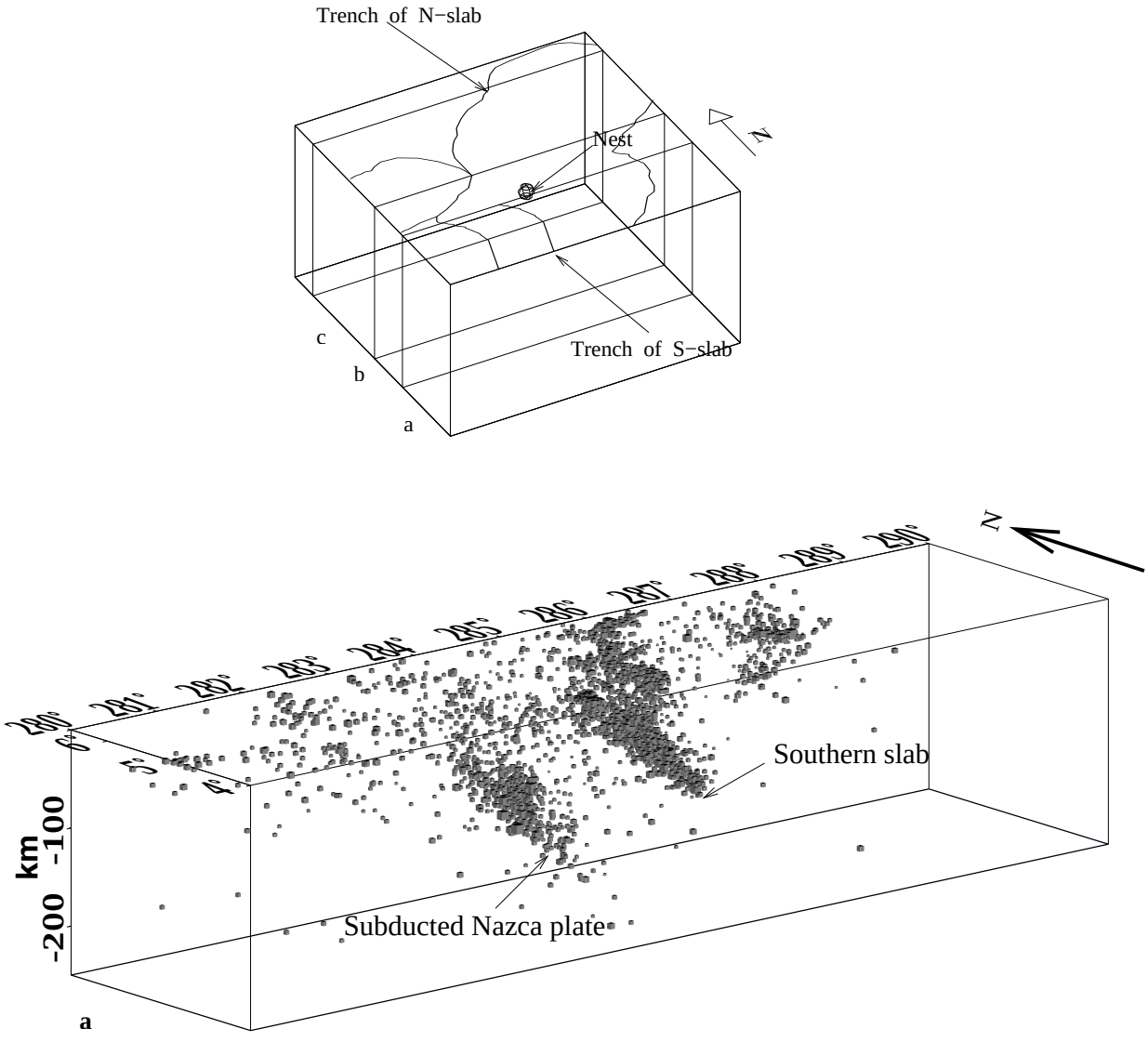

Figure 2: The index shows the location of the 3D sections. (a) The southern slab, (b) the Bucaramanga nest and (c) the northern slab. It is clear that the southern slab differs from the subducted Nazca plate. The line in the Bucaramanga nest shows the dip angle of the Bucaramanga nest.

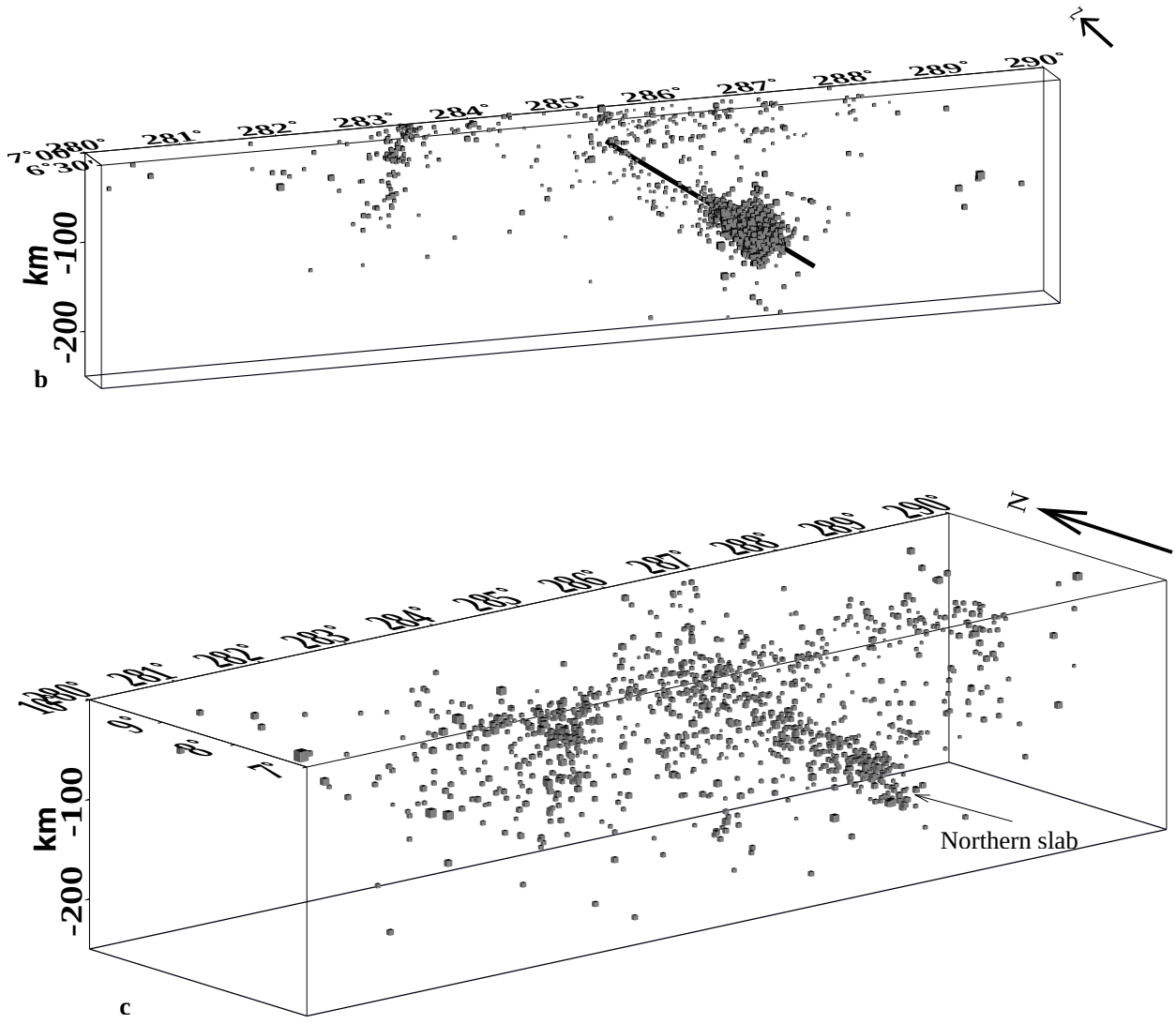

Figure 3: Continued. 2

Table 1: The fault plane solutions based on Harvard CMT catalog and the percentage of CLVDs for the earthquakes inside the Bucaramanga nest.

Date	Lon.	Lat.	Dep.	Str1	Dip1	Rake1	Str2	Dip2	Rake2	%non-DC
14/01/79	-73.21	6.85	157	261	8	-29	20	86	-97	44
11/03/79	-73.32	7.03	158	118	40	170	216	83	51	51
15/08/80	-73.12	6.67	166	257	15	-2	349	89	-105	11
29/08/83	-72.97	6.64	156	278	34	18	173	80	123	53
15/06/89	-73.09	6.87	157	109	8	-173	12	89	-82	12
03/12/90	-72.95	6.78	158	315	21	71	155	70	97	71
31/12/92	-72.96	6.74	154	41	42	124	178	56	63	8
10/12/94	-72.85	6.89	164	45	42	121	186	55	65	47
01/01/97	-72.91	6.89	164	126	48	146	240	66	47	60
08/11/99	-73.15	6.90	160	54	38	152	167	73	55	25
19/11/01	-72.90	6.74	154	324	73	-9	56	82	-162	25
18/06/04	-73.01	6.82	151	353	36	143	114	69	60	6
03/10/04	-73.04	6.83	172	148	64	-170	54	81	-27	15

2.4. Discussion on focal mechanisms earthquakes inside the Bucaramanga nest

The focal mechanism of intermediate depth earthquakes, in depth range 145-180 km, in Colombia are shown in Figure 4. In order to have more accurate distribution of earthquakes, the earthquakes' locations are chosen from the Engdahl's database (Engdahl & Villasenor, 2002). Table 1 shows information about the earthquakes just inside the Bucaramnga nest based on Harvard catalog.

Majority of the reported mechanisms have significant non-double couple component, which deserve consideration (Table 1). The percentage of CLVD is defined as 200 times of the ratio of the smallest and the largest (absolute) eigenvalue of the deviatoric moment tensor (Randall & Knopoff, 1970; Sipkin, 1986*a*,*b*). Clearly, the reported CMTs from Harvard catalog indicate variation in the earthquakes mechanism. In fact it was variation of focal mechanism of micro earthquakes in this nest, which led Schneider *et al.* (1987) and Shih *et al.* (1991) towards the idea that the Bucaramanga nest was created as a result of magma intrusion and migration, which would be followed by volcanic activ-

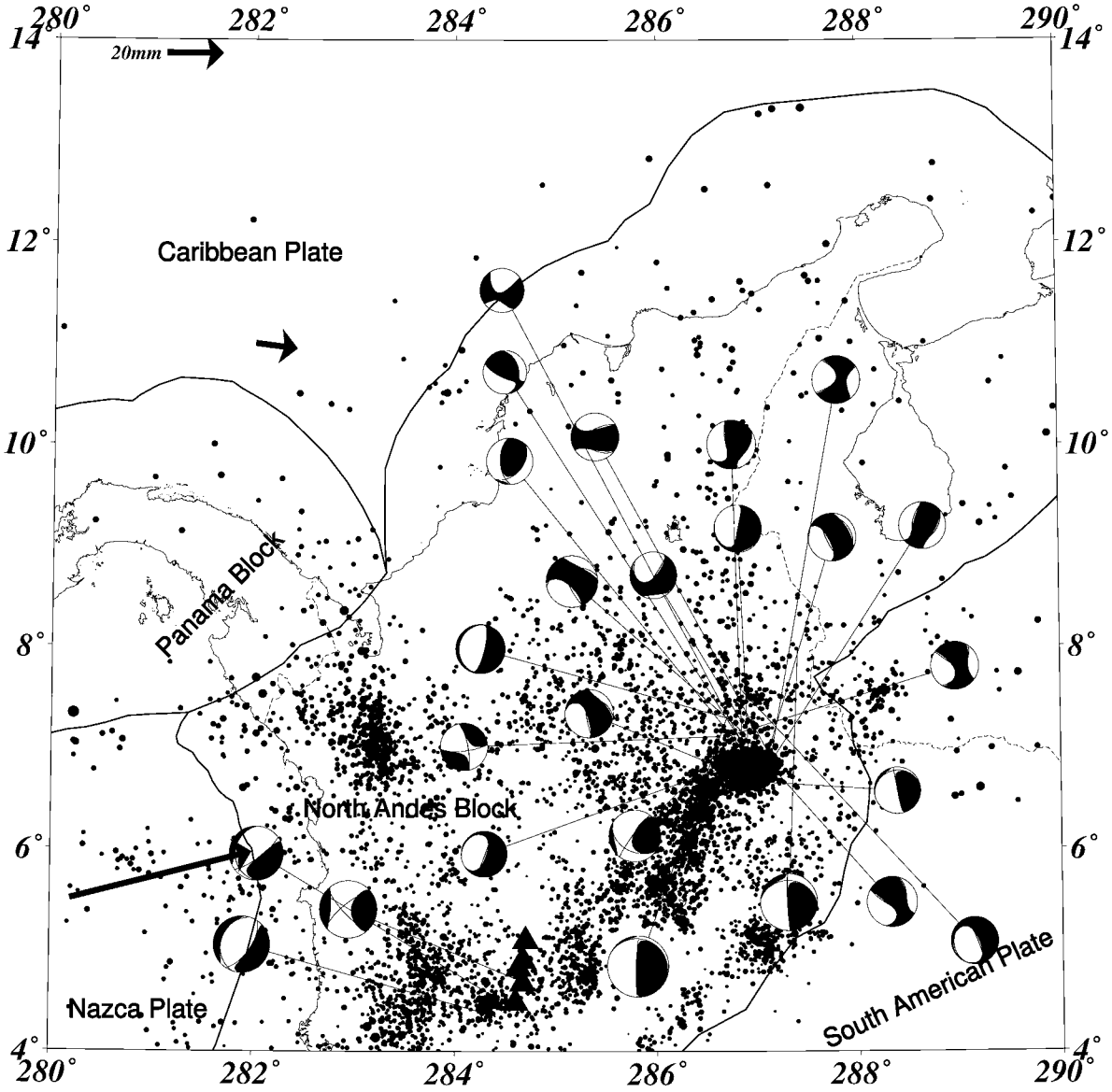

Figure 4: The Harvard CMT solutions for the earthquake in the depth interval of 145-175 km in Colombia. The location of earthquakes are determined using Engdahl's database (Engdahl & Villasenor, 2002).

ity. Indeed, this ideology can also explain the observed non-double couple components in the nest, since these type of events can usually be related to volcanic activity (Stien & Wysession, 2003). In general CLVDs can address complexity in the source of the earthquakes (Aki, 1979; Kikuchi & Kanamori, 1991; Kikuchi *et al.*, 1993). However no volcanic activity can be observed above or even around the Bucaramanga nest. On the other hand, the depth of the nest is about 150 km, which is deeper than the appropriate depth (100 km) for partial melting in the mantle wedge (Kearey & Vine, 1996). Cortes & Angelier (2005) have studied the focal mechanism stress inversion in Colombia and inside the Bucaramanga nest. The result of their study show that σ_3 has a dip angle of about 50° in the area of the Bucaramanga nest. By assuming a dip angle of about 50° for the Caribbean plate when it subducts into the asthenosphere, they proposed that the Bucaramanga nest may consequently be considered as a result of down dip tension and possible active tearing of the Caribbean slab. We compared the mechanism of the earthquakes in the Bucaramanga with the Vrancea and the Hindu Kush nests. The Vrancea nest is well known to have been created as a result of slab break off (Sperner *et al.*, 2001). The nature of the Hinsu Kush nest is explained by collision of two slabs from opposite directions (Fan *et al.*, 1994). According to Harvard CMT solution, the variation in the mechanism of earthquakes cannot be observed in the Vrancea and Hindu Kush nests. The vrancea nest also does not experience the earthquake with high percentage of CLVDs as the Bucaramanga nest does. Also, the mechanism of micro earthquakes in Vrancea nest are in agreement with the mechanism of larger earthquakes. However, the earthquakes with high percentage of CLVDs are present in the Hindu Kush nest. Further, the continuous seismic activity that can be observed in the south and the north of the Bucaramanga nest, is not apparent in the Vrancea nest. In addition neither our seismic observation nor the tomographic image of Van der Hilst & Mann (1994) can confirm such a steep dip angle for the Caribbean slab.

Reconsidering the focal mechanism of earthquakes in the nest shows that about 25%

of the earthquakes have normal mechanism. Normal faults in general can be observed at deep depth, where slab faces with increased resistance to further penetration into the mantle (Richardson & Jordan, 2002). However it has also been observed that in strongly coupled subduction, normal faults are the intermediate depth precursor to stages of a mature cycle of earthquake (Dmowska *et al.*, 1988; Taylor *et al.*, 1996; Zheng *et al.*, 1996). The characteristics of neither the northern nor the southern subducted slab in this particular area can be associated with strong coupling. The ultra low velocity of convergence of the northern slab and the steep dip angle of the southern slab prevent any strong coupling in the interplate interface (Ruff, 1989; Taylor *et al.*, 1996). Dmowska *et al.* (1988) have shown that the reason for the existence of normal extensional earthquakes at intermediate depths is the perturbation in slip in the contact zone within a cycle. This perturbed slip is a function of the degree of coupling and the velocity of convergence. Weak coupling and ultra slow velocity of convergence (southern and northern slab condition in this study) will produce very small of perturbed slip in the interplate interface, so the extensional stress will diminish fast with depth. Therefore we can barely observe normal faults at intermediate depth in this condition. So a mature cycle of earthquake cannot explain the observed normal faults at intermediate depths. Later we explain how collision between two slabs can perturb and modify the stress field and explain the observed variation in the mechanism of the earthquakes inside the Bucaramanga nest.

2.5. Focal mechanism stress inversion

In order to have a better understanding about the dominant stress regime inside the nest, We studied the focal mechanism stress inversion of the reported CMTs by Harvard (1979-2004) (Table 1) jointly with the published focal mechanisms prior to 1979 (Cortes & Angelier, 2005) (Table 2). Previously Cortes & Angelier (2005) used another method to investigate the dominant stress regime in whole Colombia including the Bucaramanga nest, and this research can reconfirm their result.

Table 2: Focal mechanism of earthquakes prior to 1979 (Cortes & Angelier, 2005)

Date	Lat.	Lon.	Dep.	Str1	Dip1	Rake1	Str2	Dip2	Rake2
1965/02/26	6.93	-73.05	147	1	82	27	267	40	175
1966/09/11	6.81	-72.95	162	36	60	147	144	66	39
1966/09/11	6.83	-72.97	162	38	56	151	145	67	38
1967/06/29	6.80	-73.00	161	188	82	123	290	30	14
1967/07/29	6.83	-73.01	165	12	88	-76	290	26	-171
1973/07/08	6.80	-73.00	156	146	66	28	44	64	154

In order to analyze the data, we used the software for analyses of seismicity patterns, ZMAP (ver 6.0) (Wyss & Wiemer, 2001). The inversion code was developed by Michael (Michael, 1984, 1987*a*,*b*; Michael *et al.*, 1990; Michael, 1991). In this code, the fault and auxiliary planes are assumed equally likely to be the rupture plane. The stress tensor is described by three orthogonal principal stress orientations σ_1, σ_2, σ_3 and a relative measure of stresses referred to as stress ratio given by: $\phi = (\sigma_2 - \sigma_1)/(\sigma_3 - \sigma_1)$, which represents the shape of the deviatoric stress ellipsoid (Michael, 1987*a*) . In order to find the 95% confidence region, the program finds 95% of the stress tensors that are closest to the best answer based on the normalized scalar product of two stress tensors according to formula 1 (Michael, 1987*a*), where M and N are the two tensors:

$$\frac{\sum_{i=1}^{3}\sum_{j=1}^{3} M_{ij}N_{ij}}{(\sum_{i=1}^{3}\sum_{j=1}^{3} M_{ij}^2)^{\frac{1}{2}}(\sum_{i=1}^{3}\sum_{j=1}^{3} N_{ij}^2)^{\frac{1}{2}}}. \tag{1}$$

Figure 5 and Table 3 show the result of the stress inversion in the nest. σ_1 in the area of the nest has an azimuth of 108.5° with a plunge of 16.7°. The state of stress based on stress inversion confirms that thrust faulting is the dominant mechanism. Plunge of σ_3 generally for intermediate depth earthquakes can denote the dip angle of slab. Figure (2a) shows that the dip angle of the southern slab is in good agreement with the plunge of σ_3 in the area of the nest. This observation generally agrees with the result of stress inversion by Cortes & Angelier (2005), who noted that Bucaramanga nest is experiencing down dip tension. However, this is just the results based on modrate size earthquakes. According to Schneider *et al.* (1987) , micro earthquakes in the nest with

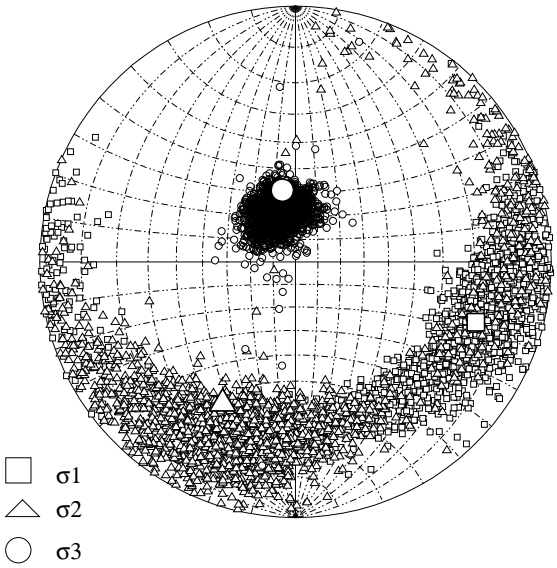

Figure 5: The results of the stress inversion in the Bucaramanga nest with 95% confidence regions for the stress tensors. σ_1 in the area of the nest has a trend of $108.5°$ with a plunge of $16.7°$, ϕ is 0.53. The trend of σ_2 is $-152.8°$ with a plunge of $26.2°$. The σ_3 has a trend of $-10.4°$ with a plunge of $58.2°$. The variance of inversion is 0.23. The dominant faulting style is thrust mechanism.

Table 3: Result of FMSI in the Bucaramnga nest. Az means azimuth and Pl means plunge. The unit for Pl, Az is degree.HRV means Harvard CMT catalog and C&A means from Cortes & Angelier (2005).

Place	σ_1		σ_2		σ_3		ϕ	Variance	No. of CMT
	Pl	Az	Pl	Az	Pl	Az			
Nest	16.7	108.5	26.2	-152.8	58.2	-10.4	0.53	0.23	13 HRV+6 C&A

their highly variable mechanism experiencing stress field different from the observed stress field based on larger earthquakes. This may imply although down dip tension is the dominent stress regim at intermediate depths due to the subduction of slab under its own weight, but in this case, it might be perturbed by the other secondary force(s) which affect the mechanism of the micro earthquakes.

2.6. Numerical simulation of slabs collision

By considering the local seismicity and tomographic image of Van der Hilst & Mann (1994) in the northeast of Colombia, we propose the scenario of collision between two

subducted slabs at intermediate depth, as a possible explanation for existence of the Bucaramanga nest. Here, we used a 3D Finite Element (FE) model to address the problem. Since the result of FE modelling depends on the geometry of the model, it is, therefore, important to build up a model as close as possible to the real geometry of the slabs. Here, we wrote a program which used the trace of the trench and the seismicity in the slab to make a 3D model as can be seen in Figure 6. This final model is in good agreement with the schematic block diagram obtained by Van der Hilst & Mann (1994), based on tomographic imaging. In this simulation the overriding lithosphere is not modeled, since the stress field inside the Bucaramanga nest is our main objective. Our goal is to show how collision between two slabs in time can concentrate and modify the stress field. In this simulation the subducting lithosphere considered to be elastic and the period of modelling is 10000 years which is the upper limit of having elastic behavior in the oceanic lithosphere (oceanic lithosphere relaxation time, which is the ratio of viscosity to rigidity). However this long period (10000 years) forces us to assume a fluid behavior for the asthenosphere (with a relaxation time of 36 years) (Turcotte & Schubert, 2002). The simulation has been done using Ansys-ED (2005) software, and due to limitation in the degree of freedom in Educational licence we constrain the affect of asthenosphere on the subducted lithosphere just to the hydrostatic pressure. For an elastic lithosphere we solved the equation of equilibrium and Hooke's equation. The stress-strain state of an elastic body is described as below (Shemenda, 1994):

$$\sigma_{ij} = \frac{E\nu}{(1+\nu)(1-2\nu)} I_1(\varepsilon)\delta_{ij} + \frac{E}{(1-\nu)}\varepsilon_{ij}, \tag{2}$$

where ε_{ij} is the strain tensor, $I_1(\varepsilon) = \varepsilon_{ij}\delta_{ij}$ is the first invariant of the strain tensor, E and ν are the Young's modulus and the Poisson ratio, respectively. Considering the elastic behavior for the lithosphere, the age dependent elastic thickness of slabs has been considered in our simulation (McNutt & Menard, 1982). The extra weight of the crust at a depth of about 100 km due to the dehydration reaction considered and fixed

to be $\delta\rho = 200\,kgm^{-3}$(Lin & Van Keken, 2005). We have also considered the extra weight due to phase transformation, in the southern slab below 300 km and fixed its value to $\delta\rho = 100\,kgm^{-3}$(Lin & Van Keken, 2005). The mantle considered to be an inviscid Newtonian fluid, so the action of viscous drag of the mantle on the lithosphere was ignored. Based on this assumption the effect of the mantle would be constrained to the hydrostatic pressure applied to the lithosphere, at the contact surfaces. The net balance between the gravitational force and the hydrostatic pressure of the fluid mantle is calculated based on Marotta & Mongelli (1998):

$$F_{net} = \delta\rho g S\cos(\theta), \tag{3}$$

where $\delta\rho$ is the density difference between the lithosphere and the mantle, S is the thickness of the lithosphere and θ is the dip of the subducted lithosphere when it enters into the asthenosphere and g is the gravitational acceleration. We used the following scaling relations in our calculations (Shemenda, 1994):

$$\frac{E}{\rho g H} = Const., \quad \nu = Const., \quad \frac{vt}{H} = Const., \tag{4}$$

where v is the velocity of convergence, H is the thickness of the slab and t is the time. Table 4 shows the values of the physical parameters for the lithosphere and the mantle, which have been used in our calculations .

The Coulomb friction between two slabs was assumed in our simulation. Although, the two slabs are subducting at a steady rate, the stick-slip process was assumed in the area of collision. This is justified by the fact that the steady state slip releases most of the energy as aseismic creep (Dieterich, 1979), while we observe abundant seismicity in the collision zone. The dynamic friction coefficient depends on the velocity of the slip, however since in the scale of our work the velocity of the slip equals the relative velocity of convergence and is too small, the ratio of dynamic to static friction is considered to

Parameters	Value
E	$1.7 \times 10^{11}\, Pa$
ρ_{mantle}	$3270\, kgm^{-3}$
$\rho_{Lithosphere}$	$3300\, kgm^{-3}$
Age of Northern slab	$70\, myr$
Age of Southern slab	$35\, myr$
Elastic thickness of N. slab	$35\, km$
Elastic thickness of S. slab	$25\, km$
ν	0.27
Dip angle of N. slab	25°
Dip angle of S. slab	50°
g	$9.81\, ms^{-2}$
μpresented	0.5
$V_{relative}$	$5.4\, cm/yr$
t	$10000\, yr$

Table 4: Value of physical parameters used in the simulation.

be equal to 1. Based on the Coulomb law:

$$\tau = \mu\sigma_n, \tag{5}$$

We considered different values for the coefficient of friction and the results show that larger values of the coefficient of friction results in slightly higher stress build up. Below, we present the result obtained for $\mu = 0.5$. Figure 6 shows the scheme of the model and the boundary conditions in our simulation. Figure 7 show the distribution of the compressional and the tensile stress in the volume. In Figure 8, the shear stress (σ_{yz}, z is direction of collision and y is the direction of subduction) and the von Mises stress is shown. The von Mises stress is defined in equation 6:

$$\sigma_e = [\frac{1}{2}((\sigma_1 - \sigma_2)^2 + (\sigma_2 - \sigma_3)^2 + (\sigma_3 - \sigma_1)^2)]^{\frac{1}{2}}, \tag{6}$$

It can be seen that in the collision zone between the southern slab and the northern slab, the compressional stress is localized (Figure 7a), However the slabs are under tension (Figure 7b) due subduction under their own weight (Chappel & Tullis, 1977). Con-

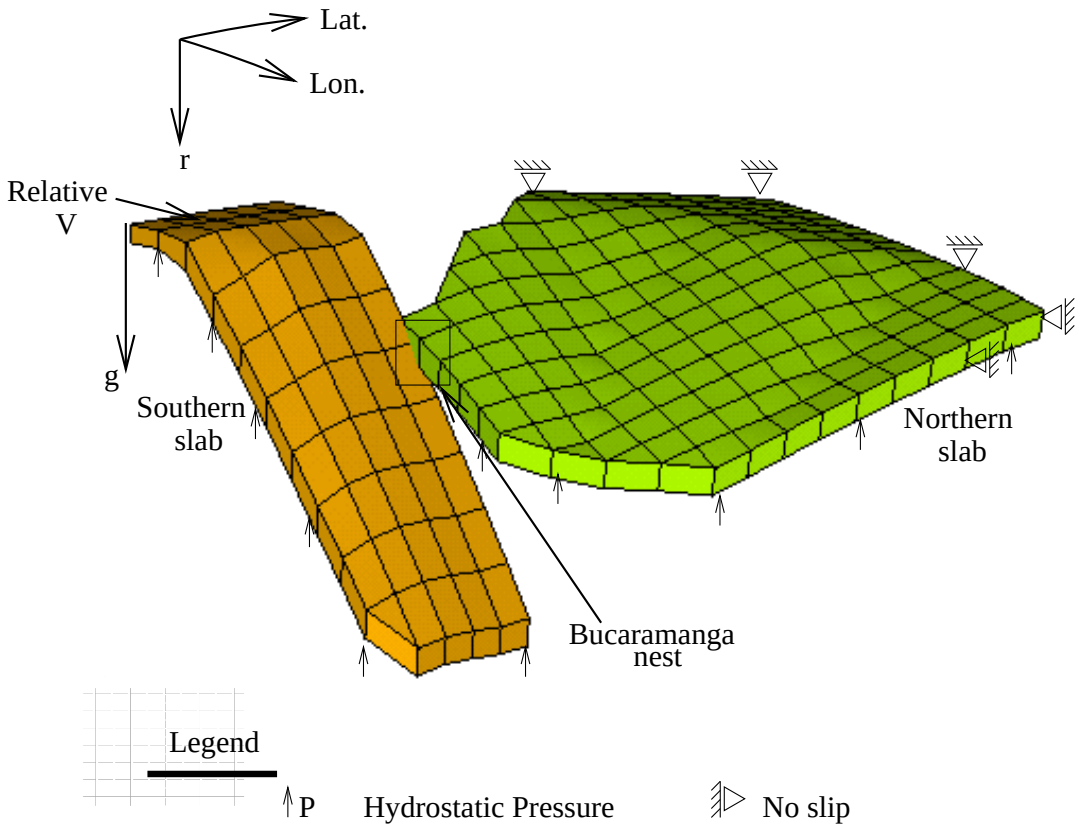

Figure 6: Scheme of the model and the boundary conditions in the simulation. P is the hydrostatic pressure, g is the gravitational acceleration. The northern slab considered to be stationary and the southern slab is subducting with the relative velocity between two slabs.

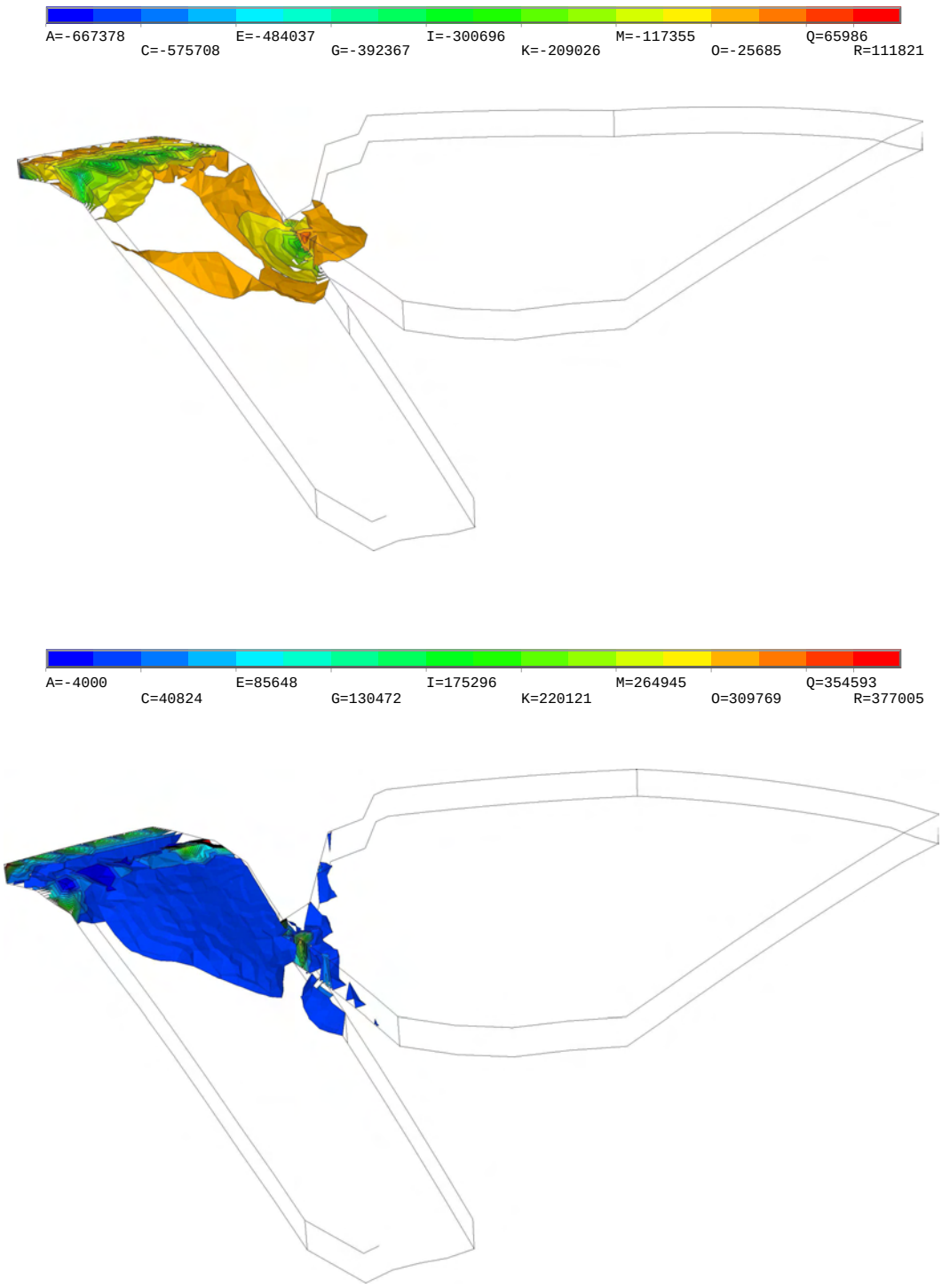

Figure 7: Volume distribution of (a) the compressional, (b) the tensile stress in the location of collision between the two slabs (the Bucaramanga nest) . The negative sign in the compression is due to the general agreement in Mechanical engineering that σ_1 is tension with positive sign and σ_3 is compression with negative sign.

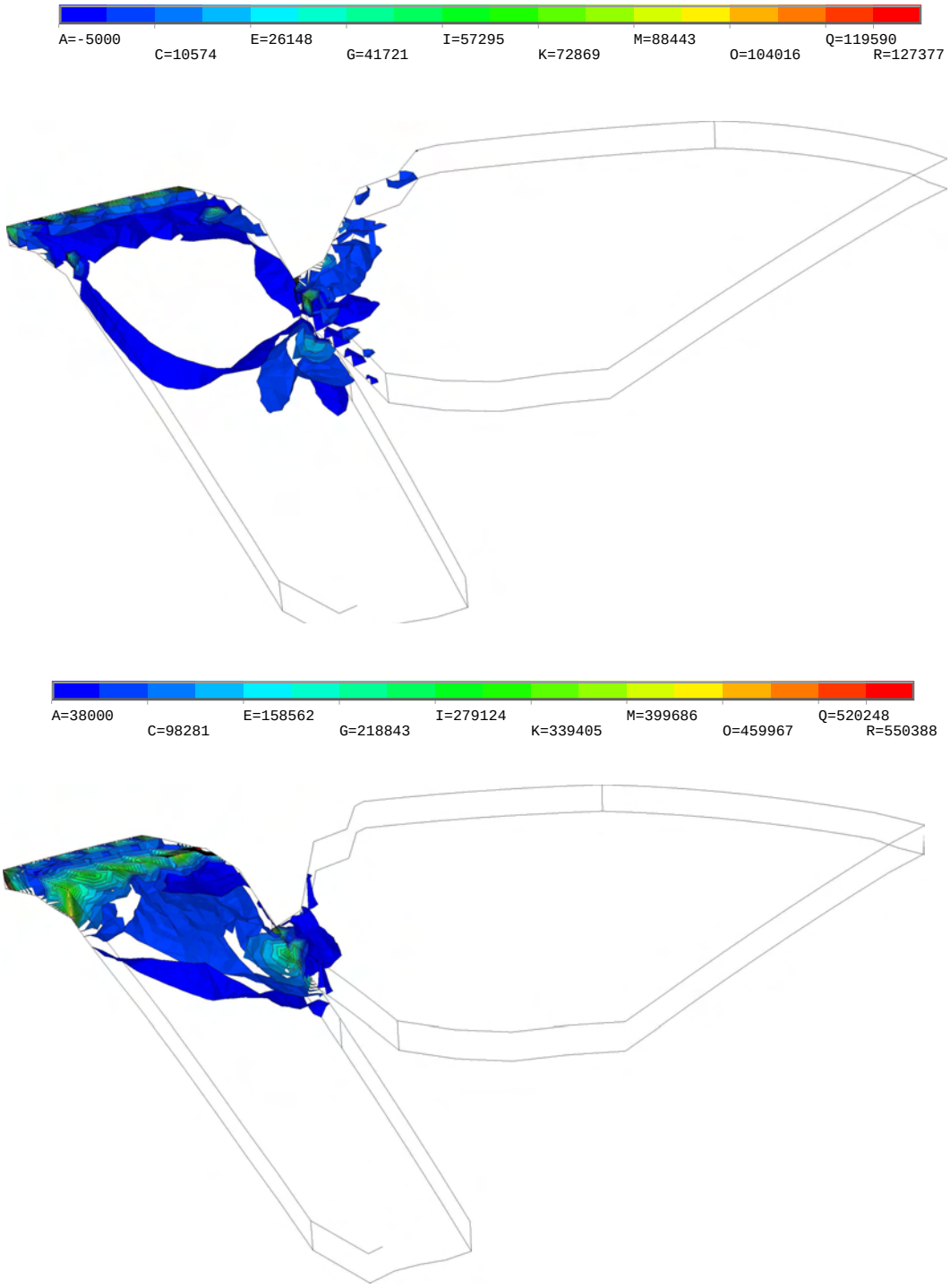

Figure 8: Volume distribution of (a) the shear stress (σ_{yz}), (b) the von Mises stress in the location of collision between the two slabs (the Bucaramanga nest).

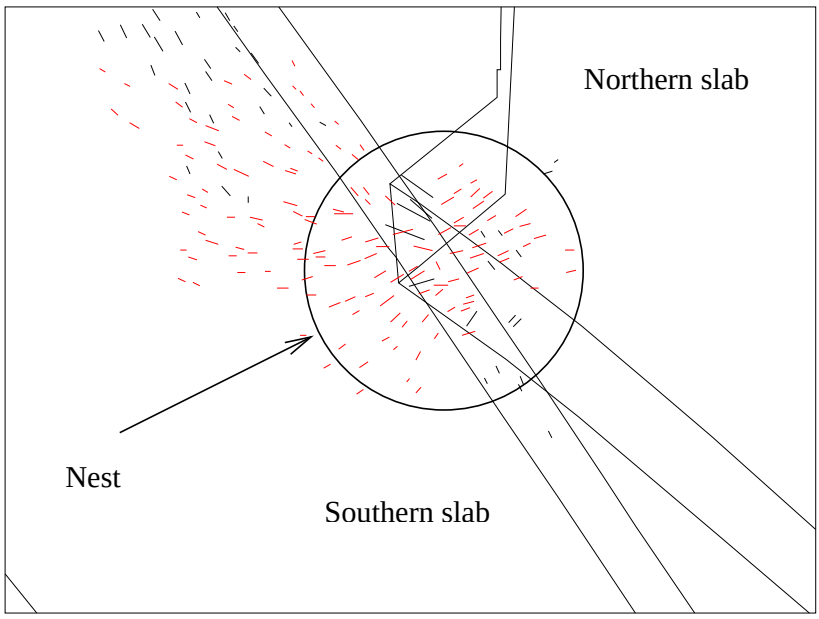

Figure 9: A sample of tensile and compressional tensors in and around the area of the Bucaramanga nest. The red lines show the compressional tensor and the black lines show the tensile tensor.

centration of the shear stress and intensified stress field can be the consequence of the collision, as can be seen in Figure 8a and b, respectively. This concentrated stress field can explain the high rate of seismic activity in the nest. Figure 9 shows how simultaneous effect of subduction and collision of slabs, create tensional and compressional stress in the area of the nest at the same time. The down dip tension in the slab can be perturbed by the down dip compression and the compressional stress in the direction of collision. This pattern of compression can explain the observation of P_{edge} and $P + I$ CLVDs (based on Frohlich *et al.* (1989) definition). Comparing the type of CLVDs in the Bucaramanga nest and the Hindu Kush can indicate that the CLVDs with normal sub event are not present in the Hindu Kush nest. According to Fan *et al.* (1994) the nature of the Hindu Kush nest can be explained by the collision between two subducted slabs. So, the difference between the type of CLVDs may be explained by the difference in the direction of collision between slabs. Direction of collision and geometry of slabs can control the direction of principal stresses and produce different type of CLVDs. Further,

the perturbed stress field in the contact zone can produce variation in the mechanism of earthquakes inside the nest.

2.7. Conclusions

The local seismicity in the northeast of Colombia reveals the existence of two slabs with two different dip angles. Our investigation shows that the dip angles of the slabs are different in the south and in the north of the Bucaramanga nest. In the north the dip angle is about 25°, while it changes to about 50° in the south. The dip angle of slab in the Bucaramanga nest is about 29°, which is in good agreement with the dip angle of the northern slab . The observed CMT solution from Harvard catalog reveals variation in the earthquakes mechanism. The eigenvalues of the deviatoric moment tensor suggest considerable non-double couple components in the source of the earthquakes. The focal mechanism stress inversion shows the tensile stress tensor in the area of the nest has a plunge of 58°. Usually the plunge of σ_3 for the intermediate depth earthquakes shows the dip angle of the slab. Here, the plunge is in good agreement with the dip angle of the southern slab. The result of FE modelling shows that the simultaneous process of subduction and collision, gives rise to concentration and variation of the stress field. The observed variation in the CMT solutions and the complexity in the source of earthquakes inside the nest is the consequence of this process. Concentrated stress field due to collision and the active process of dehydration reaction at intermediate depths can explain high release of seismic energy by micro to moderate size earthquakes in the area of the Bucaramanga nest.

Although the mechanical model that we used here can explain the characteristics of the Bucaramanga nest, but the thermal and rheological behavior of slabs have not been addressed here. Therefore a thermo-mechanical model would be more appropriate for the future investigation in this area.

Acknowledgments

We acknowledge Anibal Ojeda for providing the local data base, Kuvvet Atakan and Andrzej Kijko for reviewing the paper. We also acknowledge Hans Thybo, the editor of Tectonophysics, for providing the opportunity to improve our paper and two anonymous reviewers for their very constructive reviews. The simulations have been done with the Educational license of ANSYS provided by Geodynamics group at Earth Sciences Department, University of Bergen . We also acknowledge the ZMAP and GMT programs.

References

Aki, K. (1979). Characterization of barriers on an earthquake fault. *J. Geophys. Res.* **84**, 6140–6148.

Ansys-ED (2005). *Ansys Theory Reference*. Ansys Co.,London, UK.

Bird, P. (2003). An updated digital model of plate boundaries. *Geochemistry, Geophysics, Geosystems,* **4(3)1027**, doi:10.1029/2001GC000252.

Blot, C. (1981*a*). Earthquakes at depth beneath volcanoes, forerunners of their activities, application to White Island, New Zealand. *J. Volcanol. Geotherm. Res.* **9**, 277–291.

Blot, C. (1981*b*). Deep root of andesitic volcanoes: new evidence of magma generation at depth in the Benioff zone,. *J. Volcanol. Geotherm. Res.* **10**, 339–364.

Carr, M. J. & Stoiber, R. E. (1973). Intermediate depth earthquakes and volcanic eruptions of Fuego volcanoes in Guatemala. *EOS,* **57**, 346.

Chappel, W. M. & Tullis, T. E. (1977). Evolution of the forces that drive the plates. *J. Geophys. Res.* , 1967–1984.

Chen, P. F., Bina, C. R. & Okal, E. A. (2001). Variations in slab dip along the subducting Nazca plate, as related to stresss patterns and moment release of intermediate-depth seismicity and to the surface volcanism. *Geochemistry, Geophysics, Geosystems,* **2**, 2001GC000153.

Cortes, M. & Angelier, J. (2005). Current states of stress in the northern Andes as indicated by focal mechanisms of earthquakes. *Tectonophysics,* **403**, 29–58.

De Mets, C., Gordon, R. G., Argus, D. F. & Stein, S. (1990). Current plate motions. *Geophys. J. Int.* **101**, 425–478.

Dieterich, J. H. (1979). Modeling of rock friction:1. experimental results and constitutive equations. *J. Geophys. Res.* **84**, 2161–2168.

Dmowska, R., Rice, J. R., Lovision, L. C. & Josell, D. (1988). Stress transfer and seismic phenomena in coupled subduction zones during the earthquake cycle. *J. Geophys. Res.* **93**, 7869–7884.

Engdahl, E. R. (1977). Seismicity and plate subduction in the central Aleutians. In *Island arcs, Deep Sea Trenches and Back Arc Basins* pp. 259–271. Am. Geophys. Union, Washington, D.C.

Engdahl, E. R. & Villasenor, A. (2002). Global seismicity: 1900-1999. In *International Handbook of Earthquakes and Engineering Seismology*. Elsevier Science Ltd.

Fan, G., Ni, J. F. & Wallace, T. C. (1994). Active tectonics of the Pamirs and Karakorum. *J. Geophys. Res.* **99**, 7131–7160.

Frohlich, C., Kadinsky-cade, K. & Davis, S. D. (1995). A re-examination of the Bucaramanga Colombia, earthquake nest. *Bull. Seismol. Soc. Am.* **85**, 1622–1634.

Frohlich, C., Riedesel, M. A. & Apperson, K. D. (1989). Note concerning possible mechanisms for non-double-couple earthquake sources. *Geophys. Res. Lett.* **16**, 523–526.

Kearey, P. & Vine, F. J. (1996). *Global Tectonics*. Second edition, Blackwell Science Ltd, MA 021485018, USA.

Kikuchi, M. & Kanamori, H. (1991). Inversion of complex body waves-III. *Bull. Seismol. Soc. Am.* **81**, 2335–2350.

Kikuchi, M., Kanamori, H. & Satake, K. (1993). Source complexity of the 1988 Armenian earthquake: Evidence for a slow after slip event. *J. Geophys. Res.* **98**, 15797–15808.

Lee, W. & Lahr, H. (1987). Hypo71 (revised): a computer program for determining hypocenter, magnitude and first motion pattern of local earthquakes. *USGS open file report,* **448**, 75–311.

Lienert, B. R. & Havskov, J. (1995). HYPOCENTER 3.2: a computer program for locating earthquakes locally, regionally and globally. *Seismological Research Letters,* **66**, 26–36.

Lin, S. C. & Van Keken, P. E. (2005). Dynamics of thermomechanical plumes:2. complexity of plume structures and its implications for mapping mantle plumes.

Malave, G. & Suarez, G. (1995). Intermediate- depth seismicity in northen Colombia and western Venezuela and its relationship to Caribbean plate subduction. *Tectonics,* **14**, 617–628.

Marotta, A. M. & Mongelli, F. (1998). Flexure of subducted slabs. *Geophys. J. Int.* **132**, 701–711.

McNutt, M. K. & Menard, H. W. (1982). Constraints on yield strength in the oceanic lithosphere derived from observations of flexure. *Geophys. J. R. Astron. Soc.,* **71**, 363–394.

Michael, A. (1984). Determination of stress from slip data: Faults and folds. *J. Geophys. Res.* **89**, 11517–11526.

Michael, A. (1987*a*). Stress rotation during the Coalinga aftershocks sequence. *J. Geophys. Res.* **92**, 7963–7979.

Michael, A. (1987*b*). Use of focal mechanisms to determine stress: A control study. *J. Geophys. Res.* **92**, 357–368.

Michael, A. (1991). Spatial variation of stress within the 1987 Whittier Narrow, California, aftershock sequence: new techniques and results. *J. Geophys. Res.* **96**, 6303–6319.

Michael, A. J., Ellsworth, W. L. & Oppenheimer, D. (1990). Co-seismic stress changes induced by the 1989 Loma Prieta, California earthquakes. *Geophys. Res. Lett.* **17**, 1441–1444.

Ojeda, A. & Havskov, J. (2001). Crustal structure and local seismicity in Colombia. *J. Seismol.* **5**, 575–593.

Randall, M. J. & Knopoff, L. (1970). The mechanism at the focus of deep earhquakes. *J. Geophys. Res.* **75**, 4965–4976.

Richardson, E. & Jordan, T. (2002). Low frequency properties of intermediate focus earthquakes. *Bull. Seismol. Soc. Am.* **92**, 2434–2448.

Ruff, L. J. (1989). Do trench sediments affect great earthquake occurrence in subduction zone? *Pure Appl. Geophys.* , 263–282.

Schneider, J. F., Pennington, W. & Meyer, R. P. (1987). Microseismicity and focal mechanisms of the intermediate depth Bucaramanga nest, Colombia. *J. Geophys. Res.* **92**, 13913–13926.

Shemenda, A. I. (1994). *Subduction:Insights from Physical Modeling*. Kluwer Academic Publisher, London, U.K.

Shih, X. R., Meyer, R. P. & Schneider, J. F. (1991). Seismic anisotropy above a subducted plate. *Geology,* **19**, 807–810.

Sipkin, S. A. (1986*a*). Estimation of eathquakes parameters by the inversion of waveform data: global seismicity,1981-1983. *Bull. Seismol. Soc. Am.* **76**, 1515–1541.

Sipkin, S. A. (1986*b*). Interpretation of non-double-couple earthquake mechanisms derived from moment tensor inversion. *J. Geophys. Res.* **91**, 531–547.

Sperner, B., Lorenz, F., Bonjer, K., Hettel, S., Muller, B. & Wenzel, F. (2001). Slab break off-abrupt cut or gradual detachment? New insights from Vrancea region (SE Carpathians, Romania). *Terra Nova,* **13**, 172–179.

Stien, S. & Wysession, M. (2003). *An introduction to seismology, earthquakes and Earth structure*. Blackwell Publishing Ltd.

Taboada, A., Rivera, L. A., Fuenzalida, A., Cisternas, A., Philip, H., Bijwaard, H., Olaya, J. & Rivera, C. (2000). Geodynamics of the northern Andes: Subduction and intercontinental deformation (Colombia). *Tectonics,* **19**, 787–813.

Taylor, M. A. J., Zheng, G., Rice, J. R., Stuart, W. D. & Dmowska, R. (1996). Cyclic stressing and seismicity at strongly coupled subduction zone. *J. Geophys. Res.* , 8363–8381.

Tryggvason, E. & Lawson, JR, E. (1970). The intermediate earthquake source near Bucaramanga, colombia. *Bull. Seismol. Soc. Am.* **60**, 269–276.

Turcotte, D. L. & Schubert, G. (2002). *Geodynamics*. Second edition, Cambridge University Press, Cambridge.

Van der Hilst, R. & Mann, P. (1994). Tectonic implication of tomographic images of subducted lithosphere beneath northwestern South America. *Geology,* **22**, 451–454.

Waldhauser, F. (2001). A program to compute double difference hypocenter location. *U.S. Gelogical open file report,* , 1–113.

Waldhauser, F. & Ellsworth, W. L. (2000). A double difference earthquake location algorithm. Method and application to the northern Hayward fault, California. *Bull. Seismol. Soc. Am.* **90**, 1353–1368.

Wyss, M. & Wiemer, S. (2001). *ZMAP: A tool for analyses of seismicity pattern*. ETH, Zurich, Switzerland.

Zarifi, Z. & Havskov, J. (2003). Characteristics of dense nests of deep and intermediate-depth seismicity. *Advances in Geophysics,* **46**, 237–278.

Zheng, G., Dmowska, R. & Rice, J. R. (1996). Modeling earthquake cycles in the Shumagin subduction segment, Alaska, with seismic and geodetic constrains. *J. Geophys. Res.* **101**, 8383–8392.